

X-ray photoelectron spectroscopy of piperidinium ionic liquids: A comparison to the charge delocalised pyridinium analogues

Shuang Men^{1,2*}, Peter Licence³, Chi-Linh Do-Thanh⁴, Huimin Luo⁵ and Sheng Dai^{2*}

1 School of Material Science and Engineering
Shenyang Ligong University
Shenyang, P. R. China
110159

2 Chemical Sciences Division
Oak Ridge National Laboratory
Oak Ridge, United States
37830

3 School of Chemistry
The University of Nottingham
Nottingham, UK
NG7 2RD

4 Department of Chemistry
Joint Institute of Advanced Materials
University of Tennessee
Knoxville, United States
37996

5 Energy and Transportation Science Division
Oak Ridge National Laboratory
Oak Ridge, United States
37830

To whom correspondence should be addressed:

menshuang@hotmail.com

dais@ornl.gov

Abstract

In this study, nine piperidinium-based ionic liquids are analysed by X-ray photoelectron spectroscopy. The effect of alkyl substituent length and the nature of the anion on the electronic environment of the cation are investigated. The electronic environment of the hetero carbon and the cationic nitrogen is compared between two structurally similar cations, 1-octyl-1-methylpiperidinium ($[\text{C}_8\text{C}_1\text{Pip}]^+$) versus 1-octylpyridinium ($[\text{C}_8\text{Py}]^+$). Due to the charge delocalisation, the hetero carbon component within $[\text{C}_8\text{Py}]^+$ is more positively charged, which exhibits much higher binding energy; whilst the cationic nitrogen component is in the similar electronic environment. The impact of the charge delocalisation on the electronic environment of the anion is also compared between $[\text{C}_8\text{C}_1\text{Pip}]^+$ and $[\text{C}_8\text{Py}]^+$. It is found that for the more basic anion, the cation can significantly affect the electronic environment of the anion; for the less basic anion, such an effect concentrates on the component bearing more negative point charges.

Keywords: Piperidinium; Ionic liquids; X-ray photoelectron spectroscopy; Cation-anion interactions

Introduction

Ionic liquids (ILs) have generated considerable excitement, ascribed to their liquid nature and negligible volatility. Being composed of cations and anions, they have shown many characteristic properties, *i.e.* low melting point, high thermal stability and high conductivity, and therefore been attractive for many practical applications.¹⁻⁷ It has been concluded that by simply changing the cationic and/or anionic constituent, the physicochemical properties of ILs can be effectively tuned.

Piperidinium has been the most versatile family in applications next to imidazolium and pyridinium. Due to the lack of more acidic protons, piperidinium ILs often show higher thermal stability than imidazolium or pyridinium ILs.^{8, 9} When compared to their structurally similar charge delocalised pyridinium analogues, piperidinium ILs often show higher melting points. For example, the melting point for $[\text{C}_4\text{C}_1\text{Pip}]\text{Br}$ is 514 K,⁸ which is 136 K higher than that of $[\text{C}_4\text{Py}]\text{Br}$.¹⁰ However, for a specific case, *i.e.* switching the anion of the above two ILs to the larger delocalised bis (trifluoromethanesulfonyl)imide ($[\text{Tf}_2\text{N}]^-$), the melting point of $[\text{C}_4\text{C}_1\text{Pip}][\text{Tf}_2\text{N}]$ is found 48K below that of $[\text{C}_4\text{Py}][\text{Tf}_2\text{N}]$.¹¹ Apart from those, piperidinium ILs also show higher viscosity^{8, 12, 13} and wider electrochemical windows,^{14, 15} compared to imidazolium or pyridinium ILs. All the above properties have made piperidinium ILs potentially useful particularly in electrochemical applications.

To date, X-ray photoelectron spectroscopy (XPS) has been accepted as an effective tool to investigate ionic liquid-based systems.^{16, 17} The focus of research effort in the area of ultrahigh vacuum (UHV) characterisation has been upon a host of families of ILs, including imidazolium,^{18, 19} pyridinium,²⁰ pyrrolidinium,^{21, 22} ammonium,²³

guanidinium²⁴ and phosphonium.^{23, 25} The analysis initially includes the calculation of surface composition of ILs, the identifying of a certain component present in an ionic liquid, and the distinguishing of subtle change in electronic environment for either a cation- or an anion-based component. The scope of such a research topic is later extended to the investigation of the cation-anion interactions, which have also been probed by NMR²⁶ and Kamlet-Taft parameters.²⁷ The study of the cation-anion interactions of ILs aids proper understanding of their physicochemical properties.

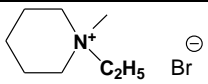
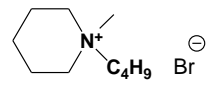
In this work, XPS is used to analyse nine piperidinium-based ILs. The effect of the alkyl chain length on the electronic environment of the cation is investigated by varying n from 2 to 12. It is found that the charge-transfer effect from the anion to the cation and the inductive effect from the alkyl substituent can both affect the electronic environment of the cation-based components, *i.e.* N_{cation} 1s. The C_{hetero} 1s binding energy is compared between [C₈C₁Pip]⁺ and [C₈Py]⁺. Due to the charge delocalisation, the hetero carbon component within [C₈Py]⁺ is more positively charged, which exhibits much higher binding energy. The charge delocalisation for [C₈Py]⁺ seems to affect the electronic environment of the nitrogen centre in a similar magnitude with the inductive effect of the additional methyl group for [C₈C₁Pip]⁺. It shows that the cationic N 1s binding energy is identical for [C₈C₁Pip]⁺ and [C₈Py]⁺. The impact the cation on the electronic environment of the anion is also studied. It concludes that for the more basic anion, *i.e.* Br⁻, the binding energy shift of Br 3d_{5/2} is noticeable (more than 0.2 eV); for the less basic anion, *i.e.* [Tf₂N]⁻, such a change in electronic environment is found concentrated on O 1s.

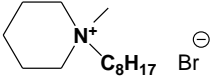
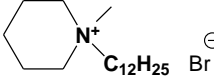
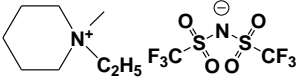
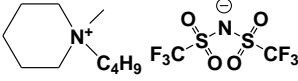
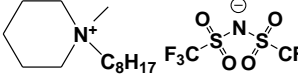
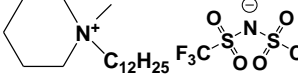
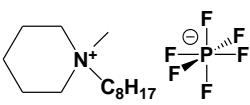
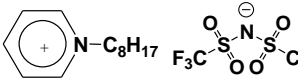
Experimental

Materials

All chemicals were purchased from Sigma Aldrich and were used as received. Ionic liquids investigated in this study were prepared in our laboratory using established synthetic protocols, and were characterised by NMR recorded on a JEOL 400YH spectrometer as solutions in DMSO-*d*₆. The procedures of synthesis of ionic liquids, NMR data and XP spectra of ionic liquids are demonstrated in detail in Electronic Supplementary Information.

Table 1 All piperidinium ionic liquids studied in this paper.

Abbreviation	Structure	Name
[C ₂ C ₁ Pip]Br		1-Ethyl-1-methylpiperidinium bromide
[C ₄ C ₁ Pip]Br		1-Butyl-1-methylpiperidinium bromide

[C ₈ C ₁ Pip]Br		1-Octyl-1-methylpiperidinium bromide
[C ₁₂ C ₁ Pip]Br		1-Dodecyl-1-methylpiperidinium bromide
[C ₂ C ₁ Pip][Tf ₂ N]		1-Ethyl-1-methylpiperidinium bis (trifluoromethanesulfonyl)imide
[C ₄ C ₁ Pip][Tf ₂ N]		1-Butyl-1-methylpiperidinium bis (trifluoromethanesulfonyl)imide
[C ₈ C ₁ Pip][Tf ₂ N]		1-Octyl-1-methylpiperidinium bis (trifluoromethanesulfonyl)imide
[C ₁₂ C ₁ Pip][Tf ₂ N]		1-Dodecyl-1-methylpiperidinium bis (trifluoromethanesulfonyl)imide
[C ₈ C ₁ Pip][PF ₆]		1-Octyl-1-methylpiperidinium hexafluorophosphate
[C ₈ Py][Tf ₂ N]		1-Octylpyridinium bis (trifluoromethanesulfonyl)imide

Note: [C₈Py][Tf₂N] is also listed in this table for the comparison of the structure.

XPS Data Collection

All XP spectra were recorded using a Thermo Scientific K_α spectrometer employing a focused, monochromated Al K_α source ($h\nu = 1486.6$ eV), hemispherical analyser, charge neutraliser and a 128-channel detector. The instrument employs an oval X-ray spot. The largest spot size (long axis) is 400 microns.

All ionic liquid (IL) samples prepared in this work were purified under high vacuum at 60 °C for at least 12 h prior to use. The IL sample was firstly transferred into a load-lock of the XPS instrument as a sample droplet on a stainless sample holder. Pumping of samples was conducted to achieve $\sim 10^{-4}$ mbar. After achieving the base pressure in the load-lock, samples were maintained pumping overnight, before transferring to the main analytical chamber.

The base pressure in the main analytical chamber is below 1×10^{-9} mbar without any samples being analysed. When analysing liquid samples, the charge neutraliser is switched off which helps the maintenance of the pressure to be below $\sim 10^{-8}$ mbar. When solid samples are being analysed, the charge neutraliser is turned on. The pressure in this case is usually below $\sim 10^{-7}$ mbar. It suggests that all volatile impurities under those vacuum conditions, such as water and organic solvents, can be completely removed, leading to high purity samples.²⁸ Consequently, the comparison of binding energies derived from XP spectra is reliable.

XPS Data Analysis

CasaXPS software was used for data interpretation. A spline linear background subtraction was used. Peaks were fitted using GL (30) lineshapes: a combination of a Gaussian (70%) and Lorentzian (30%).^{29, 30} Relative sensitive factors for all elements are taken from literature.²⁹

To aid visual interpretation of the XP spectra, all spectra were normalised to the fitted area of the cationic N 1s peak of [C₈C₁Pip][Tf₂N], simply because the cationic nitrogen atom is present in all ionic liquids in the same amount.

For $n = 8$, C_{aliphatic} 1s component was selected as an internal reference and was set to 285.0 eV for the purpose of charge correction. For other n values, N_{cation} 1s was charge corrected to the value that obtained for C₈-based analogues within a definite anion family.^{18, 21} XP spectra for [C₈Py]⁺ ILs are not measured in this study, but are available in a previous paper published by our group.²⁰

Results and discussion

Sample purity

The sample purity of ILs is confirmed by semi-quantitative analysis from XPS. The experimental surface composition for each IL is calculated from high resolution XP spectra, according to the relative sensitivity factor for each element taken from literature.²⁹ Table 2 demonstrates the surface composition for each of the IL studied in this paper. In order to give a visual comparison, the nominal stoichiometry is also included. Taking into account the error of semi-quantitative analysis from XPS, it suggests that the experimental surface composition is the same with the nominal one calculated from the empirical formulae, for each of the IL in this study.

Table 2 Experimental (calculated from XPS) and nominal stoichiometry for all ionic liquids studied in this paper

Ionic Liquids	RSF ²⁹	C 1s	N 1s	F 1s	O 1s	S 2p	P 2p	Br 3d
		0.278	0.477	1.000	0.780	0.668	0.486	1.055
[C ₂ C ₁ Pip]Br	Measured	8.5	0.8					0.7
	(Nominal)	(8.0)	(1.0)					(1.0)
[C ₄ C ₁ Pip]Br	Measured	10.3	0.9					0.8
	(Nominal)	(10.0)	(1.0)					(1.0)
[C ₈ C ₁ Pip]Br	Measured	14.3	0.9					0.8
	(Nominal)	(14.0)	(1.0)					(1.0)
[C ₁₂ C ₁ Pip]Br	Measured	18.3	0.9					0.8
	(Nominal)	(18.0)	(1.0)					(1.0)
[C ₂ C ₁ Pip][Tf ₂ N]	Measured	10.6	2.0	6.0	3.7	1.7		
	(Nominal)	(10.0)	(2.0)	(6.0)	(4.0)	(2.0)		

[C ₄ C ₁ Pip][Tf ₂ N]	Measured	12.7	2.2	5.8	3.7	1.7
	(Nominal)	(12.0)	(2.0)	(6.0)	(4.0)	(2.0)
[C ₈ C ₁ Pip][Tf ₂ N]	Measured	16.7	2.0	5.9	3.6	1.8
	(Nominal)	(16.0)	(2.0)	(6.0)	(4.0)	(2.0)
[C ₁₂ C ₁ Pip][Tf ₂ N]	Measured	20.9	1.8	5.8	3.8	1.7
	(Nominal)	(20.0)	(2.0)	(6.0)	(4.0)	(2.0)
[C ₈ C ₁ Pip][PF ₆]	Measured	14.5	0.9	5.7		0.9
	(Nominal)	(14.0)	(1.0)	(6.0)		(1.0)

Electronic environment of the carbon regions: Fitting model

Initially, the C 1s spectrum was fitted according to an established model developed for 1-alkyl-1-methylpyrrolidinium ILs reported in literature.²¹ Figure S1 shows the fitting of the C 1s spectrum for [C₈C₁Pip][Tf₂N], wherein three components are used: C_{hetero} represents carbon atoms bonded directly to the positive charged nitrogen centre; C_{inter} represents carbon atoms which are β to the cationic nitrogen; C_{aliphatic} represents the remaining carbon atoms locating further enough from the cationic nitrogen and bonded to carbon and hydrogen atoms only. This model allows a satisfactory fitting of the C 1s region for [C₈C₁Pip][Tf₂N]. However, the above model is found to be inapplicable for either [C₈C₁Pip][PF₆] or [C₈C₁Pip]Br. As shown in Figure S2, for both cases, the binding energies for C_{inter} 1s and C_{aliphatic} 1s are electronic identical by using the three-component fitting model. Therefore, it concludes that the three-component model is not always reliable for the purpose of the C 1s spectra fitting for 1-alkyl-1-methylpiperidinium ILs (more details can be found in Electronic Supplementary Information).

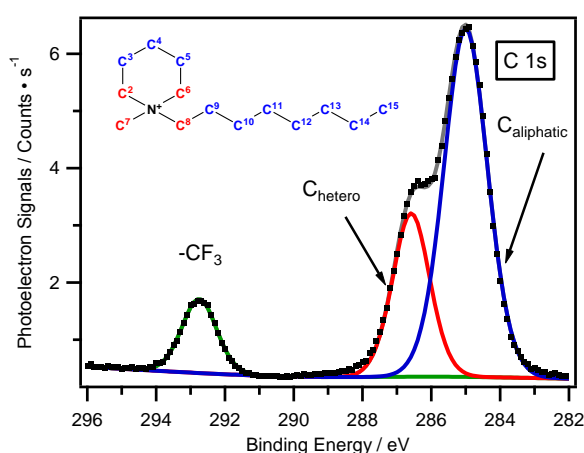


Figure 1 C 1s high resolution spectrum with fittings for [C₈C₁Pip][Tf₂N], with the structure of the cation included. A two-component model is used for the fitting: C_{hetero} 1s (C² and C⁶ to C⁸) and C_{aliphatic} 1s (C³ to C⁵ and C⁹ onwards).

Therefore, a two-component model (apart from the signal originated from -CF₃

group) is developed. Figure 1 shows the fitting procedure for [C₈C₁Pip][Tf₂N]. The structure of the cation is also included for visual comparisons. C_{hetero} is assigned to the carbon atoms bonded directly to the positively charged nitrogen; C_{aliphatic} represents to the carbon atoms bonded solely to carbon and hydrogen atoms. By constraining the area ratio of C_{hetero} : C_{aliphatic} = 4 : 10, a very satisfactory fitting can be achieved. The Full Width at Half Maximum (FWHM) ratio of C_{aliphatic} : C_{hetero} is ~1.2, as the aliphatic component is actually an overlap of more carbon signals, which produces a characteristic broader feature.^{31,32} When varying *n* values, simply changing the constraint of area ratio to C_{hetero} : C_{aliphatic} = 4 : (*n*+2), where *n* = 2-12, satisfactory fittings can be obtained.

[C_{*n*}C₁Pip]Br, where *n* = 2-12, and [C₈C₁Pip][PF₆] contain no -CF₃ group in the structure. Therefore, only the unresolved cation-based doublet C 1s peak can be observed. However, the same fitting procedure is also applicable for these ILs.

Effect of alkyl chain length on the aliphatic C 1s binding energies

In order to investigate the effect of alkyl chain length on C_{aliphatic} 1s binding energies, two families of ionic liquids are employed: one of the least basic anions, *i.e.* [Tf₂N]⁻, and Br⁻, which is a typical more basic anion. Figure 2 shows the C 1s XP spectra for these two IL families.

As demonstrated in Figure 2a, for [Tf₂N]⁻, there is an apparent shift of C_{aliphatic} 1s binding energy towards higher value, along with the decreasing of the alkyl chain length, *i.e.* from dodecyl to ethyl. When *n* = 4, the C_{aliphatic} 1s binding energy is found at 285.2 eV, which is 0.2 eV higher than that for *n* = 8. This is because the alkyl carbons present in [C₄C₁Pip]⁺ locates more closed to the positively charged nitrogen. Therefore, the inductive effect from alkyl chain to the positive headgroup leads to the decrease of the electron density on the alkyl carbon component, which subsequently shows higher binding energy. As the alkyl chain length decreases from butyl to ethyl, the C_{aliphatic} 1s binding energy is further increased to 285.3 eV. It must be noted that when *n* = 12, the C_{aliphatic} 1s binding energy is 284.9 eV, which is 0.1 eV lower than that for *n* = 8. Since the experimental error associated with XPS is of the order ± 0.1 eV, a noticeable change in binding energy should be no less than 0.2 eV. Therefore, it suggests that when increasing *n* value from 8 to 12, the electronic environment of C_{aliphatic} 1s component is not changed. This observation is in good agreement with the conclusion that has been made for pyridinium ionic liquids.²⁰ As a result, it is concluded that the electronic environment of C_{aliphatic} 1s component is always identical when *n* ≥ 8.

From another point of view, for more basic anions, *i.e.* Br⁻, the C_{aliphatic} 1s binding energy is always identical by varying *n* from 2 to 12, as shown in Figure 2b. It has been accepted that the C_{aliphatic} 1s binding energy is determined by two sets of effect: the inductive effect from the alkyl substituent towards the cation headgroup and the cation-anion interactions through charge-transfer from the anion to the cation. In the

case of more basic anions, cations and anions are tightly paired leading to a weak inductive effect. Therefore, the changing of alkyl chain length cannot affect the $C_{\text{aliphatic}}$ 1s binding energy. However, in the case of less basic anions, the charge-transfer effect is negligible which causes an intense inductive effect. As a result, noticeable changes in electronic environment of the aliphatic carbon component can be observed.

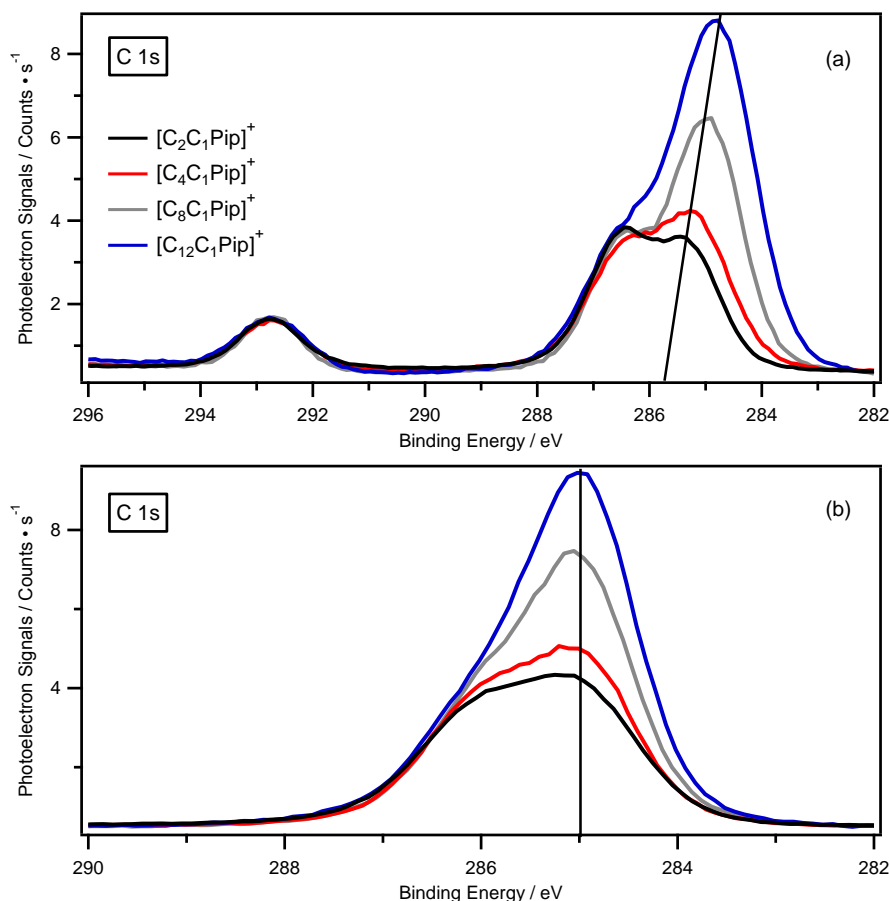


Figure 2 C 1s XPS spectra for (a) $[C_nC_1\text{Pip}][\text{Tf}_2\text{N}]$ and (b) $[C_nC_1\text{Pip}]\text{Br}$, where $n = 2-12$.

Electronic environment of the nitrogen regions: Impact of the anion

Figure 3 illustrates the N 1s spectra for $[C_8C_1\text{Pip}][\text{Tf}_2\text{N}]$, $[C_8C_1\text{Pip}][\text{PF}_6]$ and $[C_8C_1\text{Pip}]\text{Br}$. The N_{cation} 1s binding energy for $[C_8C_1\text{Pip}][\text{Tf}_2\text{N}]$ is 402.5 eV. By contrast, one for $[C_8C_1\text{Pip}]\text{Br}$ is at 402.1 eV, which is 0.4 eV lower than that of $[C_8C_1\text{Pip}][\text{Tf}_2\text{N}]$. The N 1s binding energy for $[C_8C_1\text{Pip}][\text{PF}_6]$ is 402.4 eV, which is in between of $[C_8C_1\text{Pip}][\text{Tf}_2\text{N}]$ and $[C_8C_1\text{Pip}]\text{Br}$. It indicates that the N 1s binding energies for these three ILs follow the trend: $[\text{Tf}_2\text{N}]^- > [\text{PF}_6]^- > \text{Br}^-$. This observation is in good agreement with previous XPS investigation for other families of ionic liquids.

This phenomenon can be interpreted as below. For the more basic anion, the charge-transfer effect from the anion to the cation is significant, which leads to the increase of the electron density on nitrogen centre. Consequently, the N 1s binding energy is lower. The opposite is also true for the less basic anion.

The same trend can also be found for C_{hetero} 1s binding energy, which can be found in detail in Table 3.

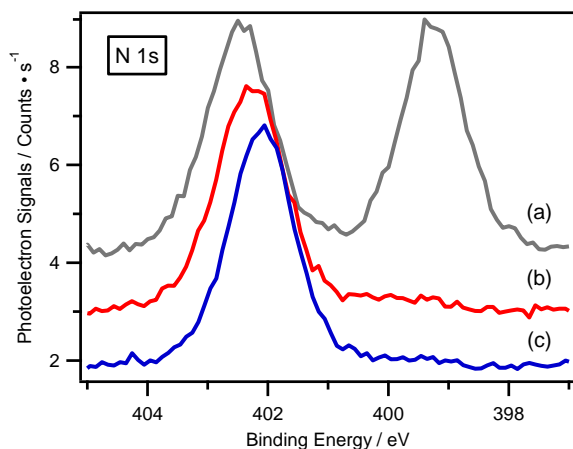


Figure 3 N 1s spectra for (a) $[C_8C_1Pip][Tf_2N]$, (b) $[C_8C_1Pip][PF_6]$ and (c) $[C_8C_1Pip]Br$.

$[C_8C_1Pip]^+$ versus $[C_8Py]^+$: Impact of charge delocalisation on hetero carbons

The positive charge delocalisation within the cation can have significant electronic influence upon the cation-based components, and subsequently the anion-based components. In the following two sections, $[C_8C_1Pip]^+$ cation is compared with a structurally similar charge delocalised cation, $[C_8Py]^+$.

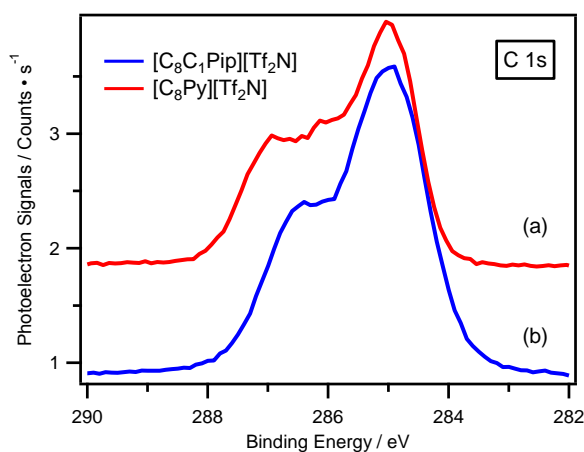


Figure 4 Cationic regions of C 1s XP spectra for (a) $[C_8Py][Tf_2N]$ and (b) $[C_8C_1Pip][Tf_2N]$.

Figure 4 compares the cationic region of C 1s XP spectra, especially the hetero carbon region, between $[C_8C_1Pip][Tf_2N]$ and $[C_8Py][Tf_2N]$. It is clear that the C_{hetero} 1s binding energy of $[C_8Py][Tf_2N]$ is much higher than that of $[C_8C_1Pip][Tf_2N]$. Due to the positive charge delocalisation, the hetero carbon component present in $[C_8Py]^+$ is much more positively charged. However, there is no delocalisation system within the structure of $[C_8C_1Pip]^+$, leading to the reality that the positive charge is solely located on the nitrogen centre. As a result, the C_{hetero} 1s binding energy for $[C_8C_1Pip][Tf_2N]$ is found ~ 0.5 eV (0.463 eV in three decimal places) lower than that

of [C₈Py][Tf₂N].

A same binding energy shift can also be observed for Br⁻ ILs (see Table 3 for details). It suggests that by switching the cation from [C₈C₁Pip]⁺ to [C₈Py]⁺, it is feasible to tune the electronic environment of the cationic hetero carbons, with only subtle impact from the anion basicity.

However, such a shift is not measurable for N_{cation} component. As shown in Table 3, N_{cation} 1s binding energies are identical for [C₈C₁Pip]⁺ and [C₈Py]⁺ ILs, with a definite anion. Although the positive charge is delocalised over [C₈Py]⁺ cation, the nitrogen is in sp² hybridisation; whilst it is in sp³ hybridisation for [C₈C₁Pip]⁺, meaning that an additional methyl group is bonded to the nitrogen centre which gives rise to the increase of electron density of the nitrogen centre. The two sets of effect, *i.e.* charge delocalisation in the case of [C₈Py]⁺ and the inductive electron donation from the additional methyl group in the case of [C₈C₁Pip]⁺ seems to have impact in similar magnitude upon the electronic environment of the nitrogen centre. Consequently, the same (within the error) N_{cation} 1s binding energy is measured for [C₈C₁Pip]⁺ and [C₈Py]⁺ ILs.

By carefully considering the N_{cation} 1s binding energy shift, it concludes that although within the XPS experimental error, the shift is more pronounced in the case of [Tf₂N]⁻ (more than 0.1 eV; whereas ~0.0 eV for Br⁻). It has been widely accepted that the charge-transfer in ILs is dependent upon the basicity of the anion. In the case of [Tf₂N]⁻, the weak charge-transfer causes the stronger electron donation effect from the methyl group within [C₈C₁Pip]⁺ towards the cationic nitrogen centre, resulting in a more noticeable change in electronic environment, which explains the slightly large N_{cation} 1s binding energy shift between [C₈Py][Tf₂N] and [C₈C₁Pip][Tf₂N].

[C₈C₁Pip]⁺ versus [C₈Py]⁺: Impact of charge delocalisation on the anion-based components

The positive charge delocalisation makes the protons (α to the positively charged nitrogen centre) within pyridinium significantly more acidic than that present in piperdinium. As reported in the literature, when associated with the same anion, *i.e.* [Tf₂N]⁻, the Kamlet-Taft hydrogen donating ability (α) for [C₄Py]⁺ is 0.51, which is much higher than that for [C₄C₁Pip]⁺ (0.43).²⁷ The less acidic cation can have more intense shielding on the point charge transferred from the anion to the cation. The electronic environment of the anion can be subsequently tuned by varying the cation.

Figure 5 shows a comparison of XP spectra for all anion-based components between [C₈C₁Pip][Tf₂N] and [C₈Py][Tf₂N]. At first glance, it is observed that binding energies for all anion-based components of [C₈C₁Pip][Tf₂N] shift towards lower values, compared to those of [C₈Py][Tf₂N]. This is because [C₈C₁Pip]⁺ can shield more partial charges transferred from [Tf₂N]⁻, leaving the anion bearing more point negative charges. However, as the charge-transfer effect in the case of [Tf₂N]⁻ is weak, the difference in

charge shielding between $[\text{C}_8\text{C}_1\text{Pip}]^+$ and $[\text{C}_8\text{Py}]^+$ is not perfectly noticeable. After carefully considering the magnitude of the binding energy shift, it suggests that the binding energy shift for F 1s, N_{anion} 1s, C_{anion} 1s and S 2p_{3/2} is within the experimental error (as shown in Figures 4a, 4c-4e). On the other hand, a noticeable change in binding energy is found for O 1s, which is more than 0.2 eV (see Figure 4b). This observation further confirms that for the less basic anion, the charge shielding effect is more concentrated on the component bearing more point charges, *i.e.* oxygen within $[\text{Tf}_2\text{N}]^-$.³³⁻³⁵ Binding energies for all elements can be found in Table 3 in detail.

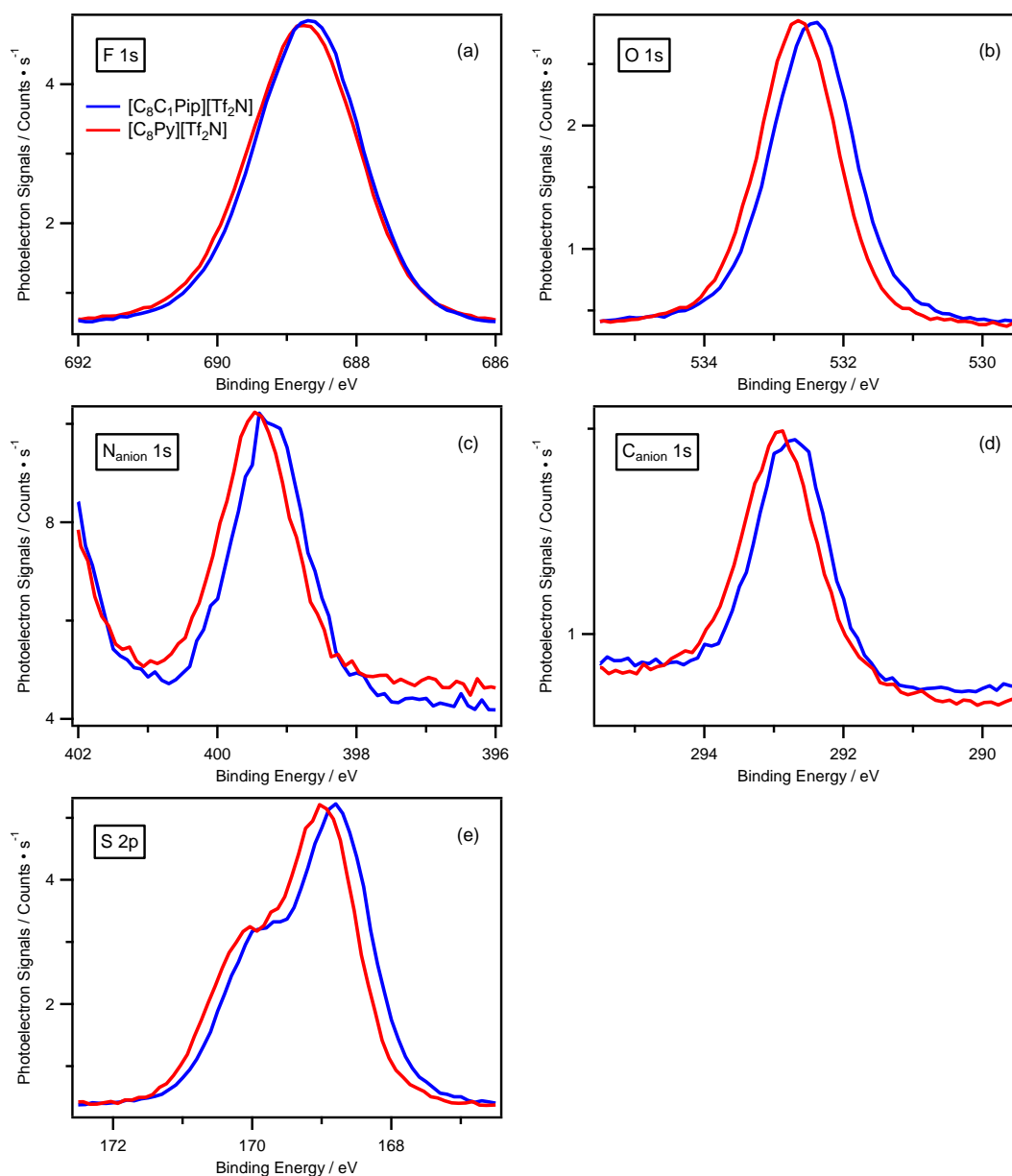


Figure 5 XPS spectra of $[\text{C}_8\text{C}_1\text{Pip}][\text{Tf}_2\text{N}]$ and $[\text{C}_8\text{Py}][\text{Tf}_2\text{N}]$: (a) F 1s, (b) O 1s, (c) N_{anion} 1s, (d) C_{anion} 1s and (e) S 2p.

For the more basic anion, *i.e.* Br, the measured binding energy shift of Br 3d_{5/2} is more than 0.2 eV, which can reflect the change in electronic environment of the anion.

Br⁻ as one of the most basic anions can transfer much more point charges to the cation. Consequently, when switching the cation from [C₈Py]⁺ to [C₈C₁Pip]⁺, the charge shielding effect is much stronger, enabling a measurable Br 3d_{5/2} binding energy shift. Figure 6 summarizes in detail the shift in binding energy for each anion-based component for the two anions.

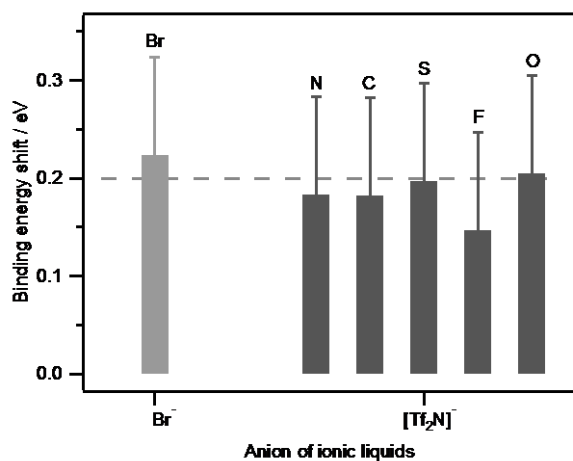


Figure 6 Binding energy shift for each anion-based component between [C₈Py]⁺ and [C₈C₁Pip]⁺ ionic liquids for the two anions.

Table 3 Binding energies in eV of all elements for all ionic liquids studied in this paper.

Ionic liquids	Binding energy / eV										
	N _{cation} 1s	C _{hetero} 1s	C _{inter} 1s	C _{aliphatic} 1s	C _{anion} 1s	N _{anion} 1s	F 1s	O 1s	S 2p _{3/2}	P 2p _{3/2}	Br 3d _{5/2}
[C ₈ C ₁ Pip][Tf ₂ N]	402.5	286.6		285.0	292.7	399.3	688.7	532.4	168.8		
[C ₈ C ₁ Pip][PF ₆]	402.4	286.5		285.0			686.5			136.4	
[C ₈ C ₁ Pip]Br	402.1	286.1		285.0							67.3
[C ₂ C ₁ Pip][Tf ₂ N]	402.5	286.6		285.3	292.8	399.2	688.7	532.4	168.8		
[C ₄ C ₁ Pip][Tf ₂ N]	402.5	286.6		285.2	292.7	399.3	688.7	532.5	168.8		
[C ₁₂ C ₁ Pip][Tf ₂ N]	402.5	286.6		284.9	292.7	399.3	688.7	532.4	168.8		
[C ₂ C ₁ Pip]Br	402.1	286.1		285.0							67.3
[C ₄ C ₁ Pip]Br	402.1	286.1		285.0							67.3
[C ₁₂ C ₁ Pip]Br	402.1	286.2		285.0							67.3
[C ₈ Py][Tf ₂ N] ²⁰	402.6	287.0	286.1	285.0	292.9	399.4	688.8	532.6	169.0		
[C ₈ Py]Br ²⁰	402.1	286.6	285.7	285.0							67.5

Conclusions

A systematic XPS study of piperidinium ionic liquids is conducted. A fitting model for the carbon region is developed. The effect of the alkyl substituent length on the $C_{\text{aliphatic}}$ 1s binding energies is demonstrated in detail by varying the alkyl chain length from ethyl to dodecyl. The impact of the anion basicity on the electronic environment of the cation-based component is investigated by employing three common anions including $[\text{Tf}_2\text{N}]^-$, $[\text{PF}_6]^-$ and Br^- . Our results show that the N 1s binding energies for these ILs follow the trend: $[\text{Tf}_2\text{N}]^- > [\text{PF}_6]^- > \text{Br}^-$. It offers a strategy for the design of ILs with desired physicochemical properties, by changing the basicity of the anion.

The impact of the charge delocalisation upon the electronic environment of the hetero carbon component is compared between $[\text{C}_8\text{C}_1\text{Pip}]^+$ and $[\text{C}_8\text{Py}]^+$. Due to the positive charge delocalisation, the C_{hetero} component present in $[\text{C}_8\text{Py}]^+$ is much more positively charged, and thus shows higher binding energy. The binding energy shift is ~ 0.5 eV. Such an effect is found with negligible impact from the anion. This observation shows good agreement with the relative stability of the two cations; piperidinium ILs are usually more stable than their structurally similar pyridinium analogues. However, for the cationic nitrogen, the binding energy is identical between $[\text{C}_8\text{C}_1\text{Pip}]^+$ and $[\text{C}_8\text{Py}]^+$. This is because within $[\text{C}_8\text{C}_1\text{Pip}]^+$, there is an inductive electron donation from the additional methyl group towards the cationic nitrogen, impacting the electron density in a similar magnitude.

The effect of the charge delocalisation on the electronic environment of the anion is also investigated by comparing $[\text{C}_8\text{C}_1\text{Pip}]^+$ versus $[\text{C}_8\text{Py}]^+$. Due to the positive charge delocalisation, $[\text{C}_8\text{Py}]^+$ is more acidic than $[\text{C}_8\text{C}_1\text{Pip}]^+$. As a result, the charge shielding effect of $[\text{C}_8\text{C}_1\text{Pip}]^+$ is stronger than that of $[\text{C}_8\text{Py}]^+$. The anion should be subsequently left bearing more negative charge. For the more basic anion, this shielding effect is reflected on the lowering of the binding energy, *i.e.* Br $3d_{5/2}$ binding energy for $[\text{C}_8\text{C}_1\text{Pip}]\text{Br}$ is found more than 0.2 eV lower than that of $[\text{C}_8\text{Py}]\text{Br}$. For the less basic anion, *i.e.* $[\text{Tf}_2\text{N}]^-$, the charge shielding effect can only affect of the electronic environment of the component bearing the most amount of point charges, *i.e.* oxygen. These findings provide insights for the tuning of ILs properties by simply modifying the cation, in particularly to the structurally similar analogue.

Acknowledgements

SM thanks Liaoning Provincial Foundation of Science and Technology (20180550482) for financial support. SM is also grateful to China Scholarship Council for the grant of a scholarship under State Scholarship Fund (201808210439) as a Visiting Scholar in Oak Ridge National Laboratory (ORNL). HML and SD are partly supported by U.S. Department of Energy, Office of Science, Basic Energy Sciences, Chemical Sciences, Geosciences, and Biosciences Division. Drs. Jun Qu and Harry Meyer

III from ORNL are acknowledged for XPS training and helpful discussions.

Reference

1. T. Welton, *Coord. Chem. Rev.*, 2004, **248**, 2459-2477.
2. V. I. Pârvulescu and C. Hardacre, *Chem. Rev.*, 2007, **107**, 2615-2665.
3. F. van Rantwijk and R. A. Sheldon, *Chem. Rev.*, 2007, **107**, 2757-2785.
4. R. A. Sheldon, R. M. Lau, M. J. Sorgedraeger, F. van Rantwijk and K. R. Seddon, *Green Chem.*, 2002, **4**, 147-151.
5. J. P. Mikkola, P. Virtanen, K. Kordas, H. Karhu and T. O. Salmi, *Appl. Catal. A-Gen.*, 2007, **328**, 68-76.
6. C. P. Mehnert, *Chem.-Eur. J.*, 2004, **11**, 50-56.
7. D. R. Macfarlane, M. Forsyth, P. C. Howlett, J. M. Pringle, J. Sun, G. Annat, W. Neil and E. I. Izgorodina, *Acc. Chem. Res.*, 2007, **40**, 1165-1173.
8. Z. Zhou, H. Matsumoto and K. Tatsumi, *Chem.-Eur. J.*, 2006, **12**, 2196-2212.
9. Y. Cao and T. Mu, *Ind. Eng. Chem. Res.*, 2014, **53**, 8651-8664.
10. J. M. Crosthwaite, M. J. Muldoon, J. K. Dixon, J. L. Anderson and J. F. Brennecke, *J. Chem. Thermodyn.*, 2005, **37**, 559-568.
11. M. Shukla, H. Noothalapati, S. Shigeto and S. Saha, *Vib. Spectrosc.*, 2014, **75**, 107-117.
12. H. Tokuda, S. Tsuzuki, M. A. B. H. Susan, K. Hayamizu and M. Watanabe, *Journal of Physical Chemistry B*, 2006, **110**, 19593-19600.
13. A. Bhattacharjee, P. J. Carvalho and J. A. P. Coutinho, *Fluid Phase Equilib.*, 2014, **375**, 80-88.
14. K. Matsumoto, R. Hagiwara and Y. Ito, *Electrochem. Solid State Lett.*, 2004, **7**, E41-E44.
15. Y. Traore, S. Legeai, S. Diliberto, G. Arrachart, S. Pellet-Rostaing and M. Draye, *Electrochim. Acta*, 2011, **58**, 532-540.
16. E. F. Smith, I. J. Villar-Garcia, D. Briggs and P. Licence, *Chem. Commun.*, 2005, 5633-5635.
17. F. Maier, J. M. Gottfried, J. Rossa, D. Gerhard, P. S. Schulz, W. Schwieger, P. Wasserscheid and H.-P. Steinrück, *Angew. Chem.-Int. Edit.*, 2006, **45**, 7778-7780.
18. I. J. Villar-Garcia, E. F. Smith, A. W. Taylor, F. Qiu, K. R. J. Lovelock, R. G. Jones and P. Licence, *Phys. Chem. Chem. Phys.*, 2011, **13**, 2797-2808.
19. Y. Liu, X. Chen, S. Men, P. Licence, F. Xi, Z. Ren and W. Zhu, *Phys. Chem. Chem. Phys.*, 2019, **21**, 11058-11065.
20. S. Men, D. S. Mitchell, K. R. J. Lovelock and P. Licence, *ChemPhysChem*, 2015, **16**, 2211-2218.
21. S. Men, K. R. J. Lovelock and P. Licence, *Phys. Chem. Chem. Phys.*, 2011, **13**, 15244-15255.

22. S. Men, B. B. Hurisso, K. R. J. Lovelock and P. Licence, *Phys. Chem. Chem. Phys.*, 2012, **14**, 5229-5238.
23. R. K. Blundell and P. Licence, *Phys. Chem. Chem. Phys.*, 2014, **16**, 15278-15288.
24. A. R. Santos, R. K. Blundell and P. Licence, *Phys. Chem. Chem. Phys.*, 2015, **17**, 11839-11847.
25. S. Men and P. Licence, *Chem. Phys. Lett.*, 2017, **681**, 40-43.
26. T. Cremer, C. Kolbeck, K. R. J. Lovelock, N. Paape, R. Wölfel, P. S. Schulz, P. Wasserscheid, H. Weber, J. Thar, B. Kirchner, F. Maier and H.-P. Steinrück, *Chem.-Eur. J.*, 2010, **16**, 9018-9033.
27. S. Spange, R. Lungwitz and A. Schade, *J. Mol. Liq.*, 2014, **192**, 137-143.
28. A. W. Taylor, K. R. J. Lovelock, A. Deyko, P. Licence and R. G. Jones, *Phys. Chem. Chem. Phys.*, 2010, **12**, 1772-1783.
29. C. D. Wagner, L. E. Davis, M. V. Zeller, J. A. Taylor, R. H. Raymond and L. H. Gale, *Surf. Interface Anal.*, 1981, **3**, 211-225.
30. D. Briggs and J. T. Grant, eds., *Surface Analysis by Auger and X-ray Photoelectron Spectroscopy*, IMPublications, Manchester, 2003.
31. G. Beamson, D. T. Clark, J. Kendrick and D. Briggs, *Journal of Electron Spectroscopy and Related Phenomena*, 1991, **57**, 79-90.
32. D. Briggs and G. Beamson, *Anal. Chem.*, 1992, **64**, 1729-1736.
33. P. A. Hunt, I. R. Gould and B. Kirchner, *Aust. J. Chem.*, 2007, **60**, 9-14.
34. S. Tsuzuki, H. Tokuda, K. Hayamizu and M. Watanabe, *J. Phys. Chem. B*, 2005, **109**, 16474-16481.
35. J. N. C. Lopes and A. A. H. Padua, *J. Phys. Chem. B*, 2004, **108**, 16893-16898.